Arch. Mech., 50, pp. 703–713, Warszawa 1998
FIFTY YEARS OF THE ARCHIVES OF MECHANICS

Coupling in thermo-mechanical wave propagation in NaF at low temperature

K. FRISCHMUTH (ROSTOCK) and V. A. CIMMELLI (POTENZA)

IN THE PRESENT PAPER we consider a linearly elastic heat conductor for which the semi-empirical heat transfer model [7] is assumed. Material functions are defined in accordance with measured parameters for NaF at 15 K. At that temperature, first and second sound waves have been observed in experiments. Both waves are reproduced by our coupled thermo-mechanical model.

1. Introduction

IN RECENT YEARS there has been considerable interest in hyperbolic models of heat conduction. The motivation for this comes from experimental observations of *heat pulses*, [1, 16, 22] at very low temperatures. The temperature is measured at one end of a specimen which is exposed to a (nearly) rectangular heat impulse at the other end. In those experiments an input pulse results in (at least) two impulses at the far end of the specimen, usually the first and the smaller one can be associated with a longitudinal mechanical wave, and the slower but greater one is a thermal wave called *second sound*.
We represent the state of the specimen by the following Fig. 1; all slices are assumed to have the same thickness in the initial state, gray level corresponds to the stress.

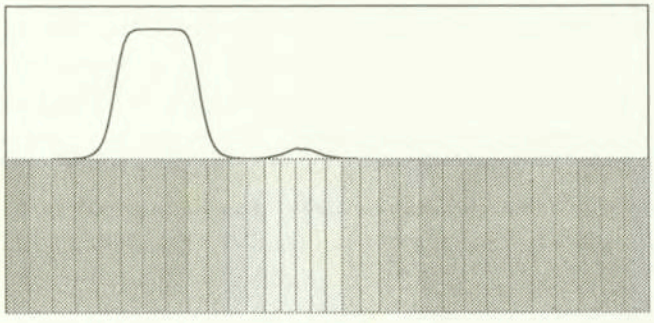

FIG. 1. Cut through deformed specimen.

Until now most models (which were developed to a level allowing numerical evaluation) concentrated on the second sound peak, disregarding the mechanical wave. There exist models for rigid heat conductors in the framework of materials

with memory [15], of rate-type materials [24], and of materials with internal state variables [18]. The quantitative differences between those models are minor, in fact for the constant coefficient case (small pulses at a constant and homogeneous background state) all they reduce to the classical Maxwell/Cattaneo/Vernotte equation

$$\tau\dot{q} + q = -\kappa\nabla\theta\,.$$

Since the second sound speed depends strongly on the background temperature, more realistic models include variable coefficients, what requires a careful thermodynamical analysis, cf. [17, 13].

Classical heat conduction theory is often criticised for the infinite wave speed it predicts [3] (Cattaneo's paradox), cf. [11] for a discussion. Here we reject the parabolic heat equation just for the simple reason that it totally failes to model the phenomenon described above. The flat curve in Fig. 2 of Sec. 4 shows the solution of the classical heat equation, which is obviously not acceptable as an approximation to the measured data, cf. [16].

The model accuracy of rigid conductor equations is obviously limited by the height of the first peak – which is absent from those models. For several experiments this lower error bound is quite large. For the internal state variable model, a pure thermal approach restricts also the possibility to obtain correct arrival times of the second sound peak, cf. [13]. Hence our present goal is to study coupled thermo-mechanical model equations.

General considerations about thermo-mechanical coupling have been published recently on the basis of the *semi-empirical heat conduction model* [5, 19]. In the present paper we present a hyperbolic system of four equations in one space variable which describes mechanical motion and heat conduction along the axis of the specimen. We will show that such a simple model can nicely reproduce the measured temperature behaviour if suitable constitutive constants are chosen. For the numerical calculations, we used values measured for NaF at 15 K, although the data come from different sources and samples of the material.

The presented model does not contain any information about the lateral motion of the specimen, hence also a peak indicated in the experimental curves as lateral mechanical wave can not be obtained. This problem has to be left to further investigation since these peaks are poorly distinguished, and the lateral mode is rather decoupled from the heat problem (at least for the isotropic case), cf. [4].

2. The coupled model

We consider here a simple 1D elastic model in the framework of classical thermo-elasticity [23] together with the basic variant of the previously studied

semi-empirical model of heat conduction. The coupling between both model components is brought about by thermal stress which acts as a source term in the mechanical subsystem, and by a heat source in the energy equation which depends on strain.

For the mechanical submodel we introduce the strain w and the velocity v as components of the state $U_{\text{mech}} = U_{\text{mech}}(x,t) = (w,v)^T$. The displacement vector is assumed to have only one non-vanishing component u – that directed along the x-axis, and this component depends only on x. We put $w = u_{,x}$ and $v = u_{,t}$. As the first balance equation we have $w_{,t} = v_{,x}$ – which is in fact, just the symmetry of the second derivatives of the displacement $u = u(x,t)$. The next balance law expresses the equation of motion, $\rho v_{,t} = \sigma_{,x}$, where σ is the stress (body forces are neglected). We adopt for the mechanical stress the linear relation $\sigma = (2\mu + \lambda)w + m\theta$, where μ and λ are Lamé constants, θ is the temperature deviation from some reference level θ_0, and m is a negative coefficient connected with thermal expansion. This gives us for the mechanical subsystem, the equations

$$w_{,t} = v_{,x}\,, \tag{2.1}$$

$$v_{,t} = c_m^2 w_{,x} + c_{mt}\theta_{,x} \tag{2.2}$$

with the mechanical wave speed $c_m = \pm\sqrt{2\mu + \lambda/\rho}$ and the coupling coefficient $c_{mt} = m/\rho$, which describes the influence of the thermal subsystem on the mechanical part.

Note that for constant temperature the above system is equivalent to the classical wave equation $u_{,tt} = c_m^2 u_{,xx}$. In the present case, however, θ has to fulfil the energy equation together with suitable constitutive equations for the heat flux.

For the thermal part of the system, the state U_{therm} is composed of just two variables, $U_{\text{therm}} = (\theta, g)^T$, where g denotes the gradient of the semi-empirical temperature β.

For the semi-empirical heat conduction theory in general, the heat flux q is given in terms of gradients of θ and β, while for β there is a kinetic equation. Taking gradients we obtain an evolution equation for $g = \nabla\beta$, cf. [17]. Throughout the present paper we restrict ourselves to the simplest case where β itself does not appear explicitly in that equation, i.e., we postulate a linear kinetic equation.

Let us further assume that θ is small enough so that we can regard heat capacity c and conductivity κ as constants (measured at θ_0). Thus we obtain for the thermal state

$$\theta_{,t} = \kappa c^{-1} g_{,x} + r, \tag{2.3}$$

$$g_{,t} = \tau^{-1}\theta_{,x} - \tau^{-1}g. \tag{2.4}$$

The first equation expresses the energy balance, the term r represents the influence of the mechanical subsystem. We found

$$r = c_{ttv}\theta_0 v_{,x}\,, \qquad c_{ttv} = m/c\,.$$

We disregard other heat sources, such as e. g. cooling through the lateral boundary – which would result in a negative source term for a 1D model.

The second equation is the extended kinetic equation in its meanwhile classical form, τ is the relaxation time; we denote $1/\tau = \gamma$ and $\kappa = K/c_0$. We observe that in the rigid conductor case ($v \equiv 0$), the above equations are equivalent to $\theta_{,tt} + \gamma\theta_{,t} = c_t^2\theta_{,xx}$, where $c_t = \pm\sqrt{\kappa/c\tau}$ is the characteristic wave speed of the thermal submodel.

The coupled system of equations becomes now

$$w_{,t} = v_{,x}\,, \tag{2.5}$$

$$v_{,t} = c_m^2 w_{,x} + c_{mt}\theta_{,x}\,, \tag{2.6}$$

$$\theta_{,t} = kg_{,x} + c_{ttv}\theta_0 v_{,x}\,, \tag{2.7}$$

$$g_{,t} = \gamma\theta_{,x} - \gamma g\,. \tag{2.8}$$

For a fully nonlinear variant – with all material parameters temperature-dependent – the energy equation should be rewritten in terms of internal energy rather than temperature. This case will be studied in a forthcoming paper.

3. Material constants and functions

Our goal is to describe a real-world situation, hence we need all relevant material constants of a material for which heat pulse experiments have been performed.

We found the best availability of measurements in the case of NaF, a cristalline solid which shows second sound effects in some interval around 16 K. In order to keep things simple we set $\theta_0 = 15$. For this temperature heat capacity, heat conductivity and second sound speed have been measured, and a temperature plot is also available [6]. So we don't use approximations but just the measured values from [16].

To complete the set of model parameters we need mass density, thermal expansion coefficient and the longitudinal wave speed. For this we use values

given in [14], concerning the speed identified from the position of the corresponding peak in the temperature plot. The following table contains all material constants we used in the numerical calculations described in the next section.

mechanical model:			
$\rho = 2.866$	$[\mathrm{g/cm^3}]$	$m = -1.1464$ E-5	$[\mathrm{g/\mu s^2/cm/K}]$
$c_m = 0.5477$	$[\mathrm{cm/\mu s}]$	$c_{mt} = -4.0$E-6	$[\mathrm{cm^2/\mu s^2/K}]$
thermal model:			
$c = 7950$	$[\mathrm{Ws/m^3/K}]$		
$\kappa = 205$	$[\mathrm{W/cm/K}]$	$c_{ttv} = -144.8$	[1]
$c_t = 0.19531$	$[\mathrm{cm/\mu s}]$		
$\tau = \kappa/c_t^2/c = 0.675986$	$[\mu s]$		
$\gamma = 1/\tau = 1.47932$	$[1/\mu s]$		

4. Numerical method

In this section we study initial-boundary value problems for the above system (2.5) - (2.8). We assume that the body is initially at equilibrium: there is no motion, no temperature gradient, no heat flux. Then, at the left-hand boundary $x = 0$, we apply a trapezoidal heat impulse. The temperature is continuously but quickly increased, then it is kept constant, and then decreased,

$$\theta = at\chi_{[0,t_1]} + at_1\chi_{[t_1,2t_1+t_2]} + a(t_1 + t_2 - t)\chi_{[t_1+t_2,2t_1+t_2]}\,.$$

Here is $2t_1 + t_2$ the total duration of the pulse, t_1 is the time needed for heating or cooling, cf. [10]. By χ we denote the characteristic functions.

At the right-hand boundary $x = l$ we "measure" the temperature $\theta(l, \cdot)$, the velocity $v(l, \cdot)$ and the strain $w(l, \cdot)$ which are caused by that impulse.

For a fast numerical solution we want to apply an explicit method with constant stepsizes, cf. [21]. Such methods as Lax-Friedrich or Lax-Wendroff schemes are available and well understood for conservation laws of the form [2]

$$u_{,t} + f(u)_{,x} = 0\,.$$

In this section we denote by $u = u(x,t)$ the state $u = (U_{\mathrm{mech}}, U_{\mathrm{therm}})^T$. In our case we have a source term $b(u)$ on the right-hand side, the system is not in divergence form.

Observe that for the isothermal case $\theta \equiv \mathrm{const}$, the mechanical subsystem has the classical form, and we obtain nice numerical results with any of the mentioned methods.

Let us explain shortly the idea of the methods for this case. We replace the flux f by a consistent numerical flux $F^{(h)}$ which depends on the step-size h of the equidistant mesh in x-direction. A time-step is then carried out according to

$$U_{n+1} = U_n - \Lambda h \Delta F^{(h)},$$

where U_n is the numerical solution at time-step n, Δ denotes the forward difference, and Λ is the ratio of time to space step-size.

Classical requirements for such methods are the consistency of the numerical flux with the analytical one, i.e. $f(u) = F^{(h)}(u, \ldots, u)$ (the numerical flux depends on the state in several nodes, for Lax-Friedrich and Lax-Wendroff on two, cf. [21]), and the CFL condition (Courant, Friedrich, Levy) which imposes a bound on the ratio Λ. The latter has to be smaller than one over the largest sound speed (here c_m) [9].

The Lax-Friedrich scheme is monotone – it does not introduce artificial oscillations – but it also introduces considerable numerical diffusion; it is only of the first order accuracy. On the other hand, the second order Lax-Wendroff scheme often shows unphysical oscillations near shocks [20].

For our mechanical problem, however, both give quite good results for appropriate Λ. We obtain the best accordance with the known analytical solution just before violating the CFL condition, i.e. with $\Lambda \approx 1/c_m$ (see Figs. 2 and 3).

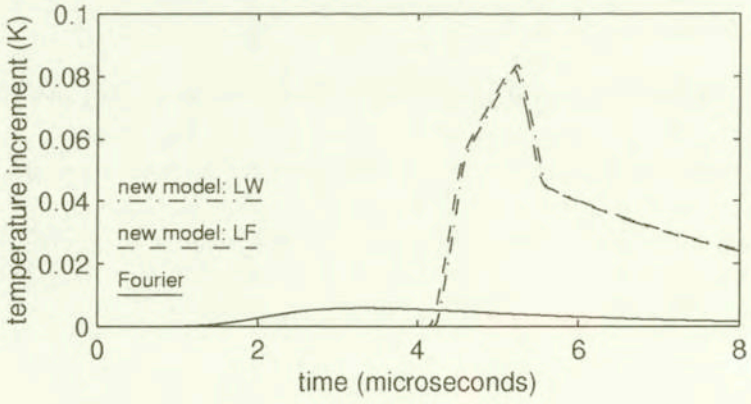

FIG. 2. Thermal submodel.

In the same manner we can consider the rigid thermal subsystem, cf. [12]. However, here we encounter already a source term which spoils the performance of the Lax-Friedrich scheme.

In order to understand that fact, we can decompose the state u in the eigenbasis of $\nabla_u f$. Then the differential part of the system is nicely diagonalized, but

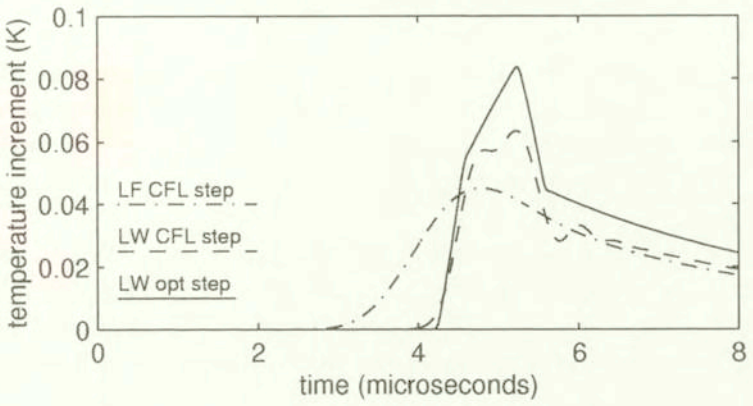

FIG. 3. Dependence on step-size and method.

there is a coupling via the right-hand side. This leads to an exponential decay of the amplitude of a pulse running into an equilibrium region. The Lax-Wendroff method (with Λ near $1/c_t$) reproduces this behaviour correctly.

For the thermo-mechanical system, the optimal step-size for the thermal subsystem is forbidden by the CFL condition (in all second-sound materials, the speed of the longitudinal elastic wave is larger than the speed of the thermal pulses).

However, the Lax-Wendroff results with a wrong Λ are still quite acceptable (Fig. 4). A method which removes the error caused by numerical diffusion is under preparation. The idea is to integrate both subsystems in their own meshes and just to exchange the coupling terms (waveform relaxation).

Let us discuss now some results for sodium fluoride (NaF) at 15 K.

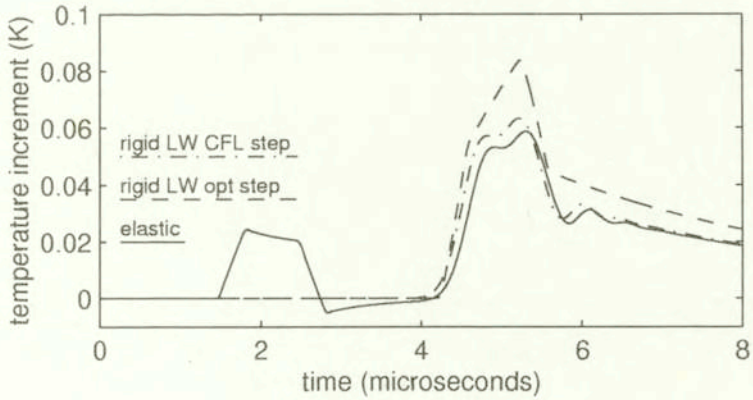

FIG. 4. Temperature at far end.

5. Results and conclusions

We omit the mechanical subsystem, and start with the rigid conductor. We compare a classical heat conductor (Fourier law) with our present second sound model. We give the temperatures at the right end of the specimen versus time as calculated by Lax-Friedrich and Lax-Wendroff schemes, with optimal step-size in Fig. 2.

Figure 2 shows so-called *arrival prints* of temperature. We can see that the classical heat conduction theory (flat curve) is obviously not applicable, and the Lax-Friedrich scheme is not distinguishable from Lax-Wendroff. On both curves we can still recognize the 4 jumps of the first derivative which come from the applied trapezoidal impulse.

A comparison between the optimal Lax-Wendroff solution and those obtained with the step-size imposed by the CFL condition for the full system shows the failure of the Lax-Friedrich method (Fig. 3).

We use 600 time steps and 110 space steps if the mechanical wave is relevant, 316 space steps otherwise. The Lax-Friedrich solution adds too much numerical viscosity, it looks like a solution to the classical parabolic equation.

Now we come to the full system. We do not apply any non-vanishing mechanical initial or boundary conditions, just a thermal pulse as in the rigid case. As a result we obtain a compression wave, combined with an increase of temperature, which travels approximately 3 times faster than the second sound pulse.

In the wake of the first pulse we see a tiny drop of the temperature level below the temperature of the environment – an observation confirmed by the experimental plots, cf. [16]. We present here the arrival situation for temperature (Fig. 4), velocity (Fig. 5) and strain (Fig. 6).

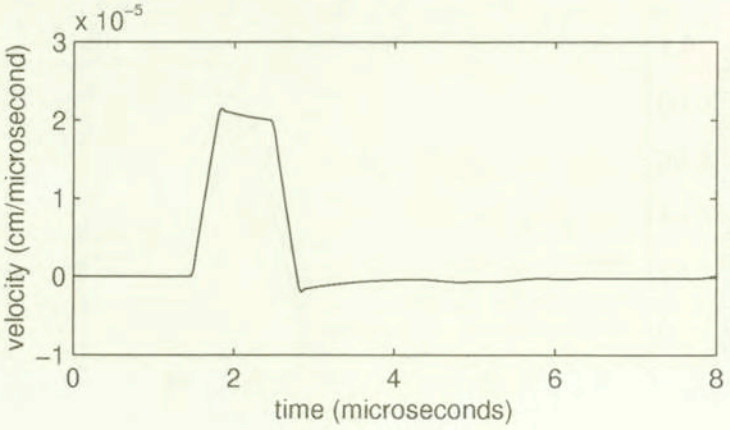

FIG. 5. Velocity at far end.

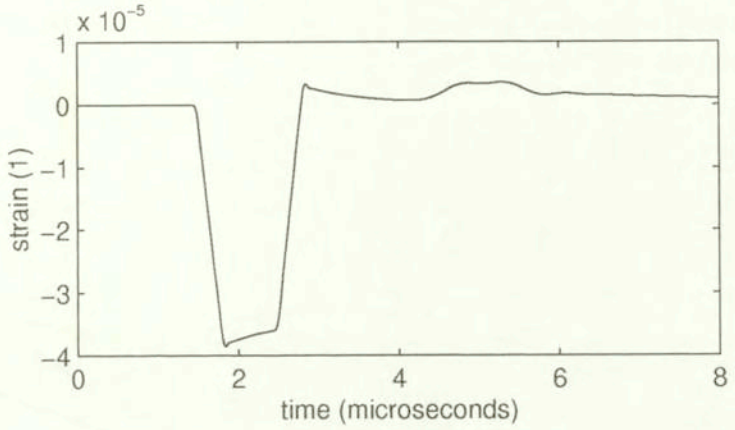

FIG. 6. Strain at far end.

We superimpose onto the plot of the temperature (Fig. 4) in the coupled model, the plots for θ as it results for the rigid conductor equations, once calculated with optimal step-sizes, and for comparison that calculated at the same mesh as in the coupled case. It is very clear that after 4 microseconds, the influence of the mechanical wave has nearly vanished. We suppose that the true solution after that time is similar to the rigid conductor solution – which is consistent with our expectation on the basis of the large difference between both wave speeds.

Finally, we visualize the result by a density plot and a 3D temperature distribution as a function of space and time, Figs. 7 and 8. The two pulses are

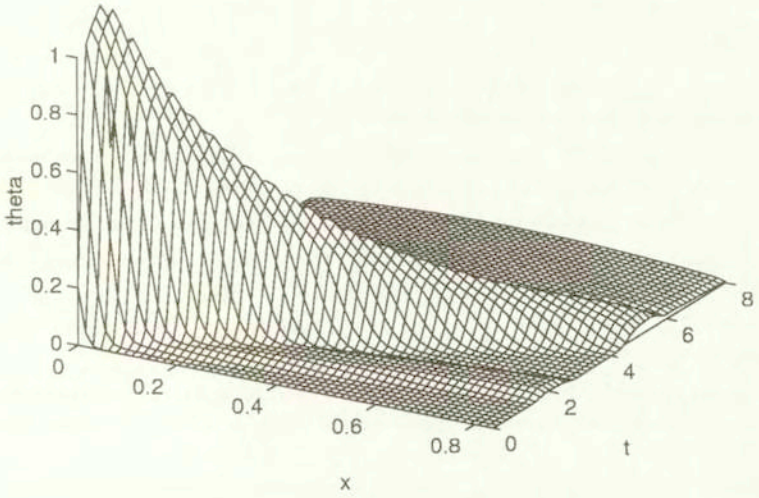

FIG. 7. 3D-plot of temperature.

clearly visible, the slopes of the isolines in the density plot are the reciprocals of the characteristic speeds c_m and c_t.

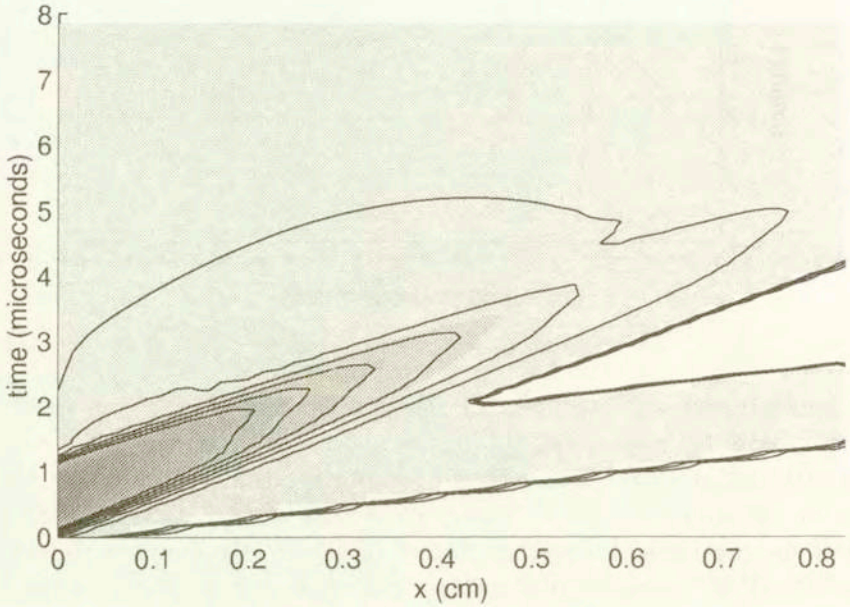

FIG. 8. Density plot: two characteristic speeds.

We hope to get an even better accordance between our numerical results and the real measurements by improving the model as well as the solver. Next steps will be the variable coefficients and more realistic boundary conditions, as well as a (negative) source term.

References

1. C. C. ACKERMAN, B. BERTAM, H. A. FAIRBANKS and R. A. GUYER, *Second sound in solid Helium*, Phys. Rev. Letters, **16**, 789, 1966.
2. R. ANSORGE, *A lecture on entropy conditions and their numerical analogues for conservation laws*, Hamburger Beiträge zur Angewandten Mathematik, B14, April 1991.
3. C. CATTANEO, *Sulla conduzione del calore*, Atti Sem. Mat. Fis. Univ. Modena, **3**, 83, 1948.
4. G. CAVIGLIA, A. MORRO, and B. STRAUGHAN, *Thermoelasticity at cryogenic temperatures*, Int. J. Non-Linear Mechanics, **27**, 2, 251–263, 1992.
5. V. A. CIMMELLI, *Thermodynamics of anisotropic solids near absolute zero*, Math. Comput. Modelling 1998 (in press).
6. V. A. CIMMELLI and K. FRISCHMUTH, *Determination of material functions through second sound measurements in a hyperbolic heat conduction theory*, Math. Comput. Modelling, **24**, 12, 19, 1996.
7. V. A. CIMMELLI and W. KOSIŃSKI, *Nonequilibrium semi-empirical temperature in materials with thermal relaxation*, Arch. Mech., **43**, 6, 753–767, 1991.

8. B. D. COLEMAN and M. E. GURTIN, *Thermodynamics with internal state variables*, J. Chem. Phys., **47**, 597–613, 1967.

9. R. COURANT, K. O. FRIEDRICHS, and H. LEWY, *Über die partiellen Differenzengleichungen der mathematischen Physik*, Math. Ann., **100**, 32–74, 1928.

10. W. DREYER and H. STRUCHTRUP, *Heat pulse experiments revisited*, Continuum Mech. Thermodyn., **5**, 3, 1993.

11. G. FICHERA, *Is the Fourier theory of heat propagation paradoxical?* Rendiconti del Circolo Matematico di Palermo, Serie II, Tomo XLI, 5–28, 1992.

12. K. FRISCHMUTH and V. A. CIMMELLI, *Numerical reconstruction of heat pulse experiments*, Int. J. Engng. Sc., **33**, 2, 209, 1995.

13. K. FRISCHMUTH and V. A. CIMMELLI, *Identification of constitutive functions and verification of model assumptions in semi-empirical heat conduction theory*, Quaderni del Dipartimento di Matematica, Potenza, Report No. 4, 1994.

14. *Gmelin handbook of inorganic and organometallic chemistry*, Springer, Berlin 1993.

15. M. E. GURTIN and A. C. PIPKIN, *A general theory of heat conduction with finite wave speeds*, Arch. Rat. Mech. Anal., **31**, 113–126, 1968.

16. R. J. HARDY and S. S. JASWAL, *Velocity of second sound in NaF*, Phys. Rev. B, **3**, 4385, 1971.

17. W. KOSIŃSKI, *Thermodynamics of continua with heat waves*, in Proc. ASME Joint Applied Mechanics and Materials Summer Meeting, UCLA 1995, AMD, **18**, 19, 1995.

18. W. KOSIŃSKI and P. PERZYNA, *Analysis of acceleration waves in materials with internal parameters*, Arch. Mech., **24**, 4, 629, 1972.

19. W. KOSIŃSKI and W. WOJNO, *Gradient generalization to internal state approach*, Arch. Mech., **47**, 3, 523, 1995.

20. P. D. LAX and B. WENDROFF, *Systems of conservation laws*, Comm. Pure Appl. Math., **13**, 217–237, 1960.

21. R. J. LEVEQUE, *Numerical methods for conservation laws*, Birkhäuser, 1992.

22. V. NARAYANAMURTI and R. C. DYNES, *Observation of second sound in bismuth*, Phys. Rev. Lett., **28**, 1401, 1972.

23. W. NOWACKI, *Thermoelasticity* [in Polish], Ossolineum, Wrocław, Warszawa, Kraków, Gdańsk 1972.

24. B. D. COLEMAN, M. FABRIZIO and D. R. OWEN, *On the thermodynamics of second sound in dielectric crystals*, Arch. Rat. Mech. Anal., **80**, 135, 1982.

DEPARTMENT OF MATHEMATICS
UNIVERSITY OF ROSTOCK
18051 Rostock, Germany
e-mail: kurt@sun2.math.uni-rostock.de
and
DEPARTMENT OF MATHEMATICS
UNIVERSITY OF BASILICATA
85100 Potenza, Italy
e-mail: Cimmelli@unibas.it

Received January 30, 1998.